



Nano-textured polydimethylsiloxane cantilever with embedded silver nanowire networks for drug screening applications

Yuyan Liu^a, Nomin-Erdene Oyunbaatar^{a,b}, Arunkumar Shanmugasundaram^{a,b},
Eung-Sam Kim^c, Bong-Kee Lee^a, Dong-Weon Lee^{a,b,d,*}

^a School of Mechanical Engineering, Chonnam National University, Gwangju 61186, the Republic of Korea

^b Advanced Medical Device Research Center for Cardiovascular Disease, Chonnam National University, Gwangju 61186, the Republic of Korea

^c Department of Biological Sciences and Research Center of Ecomimetics, Chonnam National University, Gwangju, 61186, Republic of Korea

^d Center for Next-Generation Sensor Research and development, Chonnam National University, Gwangju 61186, the Republic of Korea

ARTICLE INFO

Keywords:

AgNWs-embedded PDMS
Conductive and topographical stimulation
Improved cell maturation
Drug screening platform
Cardiotoxicity assessment

ABSTRACT

Drug-induced cardiotoxicity is the primary cause of heart failure and leading to withdrawal of drugs from the market. Although in vitro animal models are successfully used in fundamental research on heart physiology, cardiac disease, and cardiovascular drug development, the immature cardiomyocytes utilized in existing in vitro screening techniques cannot effectively replicate the natural physiology of adult cardiomyocytes. As a result, the results obtained in vivo contradict those obtained in vitro. Herein, we propose a nanotextured polydimethylsiloxane cantilever integrated with embedded silver nanowire (AgNWs-E-PDMS) to enhance cardiomyocyte maturation. The cardiomyocytes cultured on the functional PDMS cantilever exhibit an enhanced cell viability, synchronized and stable beating behavior, and Ca^{2+} transient signals and cell adhesion. The Western blot (WB) and reverse transcription polymerase chain reaction (RT-qPCR) tests also showed that connexin-43 (Cx43) protein and its gene expression in cardiomyocytes are 4.59 and 1.75 times higher than in the control group of cardiomyocytes. The performance of the cantilever-based screening platform is also verified by performing sequential drug analysis using neonatal rat ventricular myocytes (NRVM) and human-induced pluripotent stem cell cardiomyocytes (hiPSC-CMs) on nanotextured PDMS and AgNWs-E-PDMS cantilevers. We expect that the proposed cantilever device will help reduce the risk of drug-induced heart disease in the early stages of drug development.

1. Introduction

Cardiovascular disease is the leading cause of death globally. Pharmaceutical companies are researching and developing drugs to reduce mortality, but many drugs have been withdrawn from the market due to drug-induced cardiotoxicity issues [1,2]. In vitro screening technologies often show discrepancies with in vivo observations, contributing to high failure rates during preclinical trials [3–6]. The cardiomyocytes used in in vitro applications cannot accurately reflect natural physiological conditions during the drug screening process [7]. For this reason, it is necessary to develop a functional tissue engineering substrate that can better replicate natural physiological conditions to improve the accuracy of drug screening.

Several years of research on cardiovascular drug screening has provided insight into enhancing cell maturation [8,9]. Among them,

topographical stimulation and the use of conductive materials are effective approaches for improving cell maturation [10–13]. Topographical stimulation aligns cardiomyocytes and activates signaling pathways, resulting in faster maturation and the development of desired phenotypes [14,15]. Conductive biomaterials can mimic the heart's physiological conditions and enhance electrical signaling, promoting proliferation, intracellular communication, and growth of cardiomyocytes [16,17]. Deposition of thin electroconductive metal layers like gold on the culture substrate can enhance differentiation and maturation, but the formation of cracks on the metal layer can reduce reliability [18]. Conductive polymers such as polyethyleneimine and poly-L-ornithine, etc. improve adhesion and maturation but may affect cardiomyocytes depending on factors such as charge density, exposure time, and concentration [19–23].

Nanostructured semiconducting and conductive fillers are

* Corresponding author at: School of Mechanical Engineering, Chonnam National University, Gwangju 61186, the Republic of Korea.

E-mail address: mems@jnu.ac.kr (D.-W. Lee).

<https://doi.org/10.1016/j.snb.2023.134014>

Received 5 March 2023; Received in revised form 11 May 2023; Accepted 22 May 2023

Available online 23 May 2023

0925-4005/© 2023 Elsevier B.V. All rights reserved.

increasingly used in biomedical applications due to their high electrical conductivity [24–28]. Tan et al. incorporated trace amounts of silicon nanowires (SiNWs) to enhance cellular contraction and maturation [29]. However, the biocompatibility of SiNWs is not well-known, and their degradation products can affect cardiomyocytes. Carbon nanotube-PDMS, graphene-PEG, and carbon nanotube-hydrogel-based composites have been proposed to improve cell maturation but lack the mechanical properties of native heart tissue [30–34]. The utilization of gold nanowires and gold nanorods has been demonstrated to enhance cell maturation [17,35]. However, their economic feasibility remains a significant challenge when considering their widespread implementation in practical applications.

Silver nanowires (AgNWs) have high electrical conductivity (16 n Ω m), good mechanical flexibility, and a facile solution-based fabrication process, making them promising candidates for biomedical applications [24,25]. However, AgNWs tend to oxidize when exposed to air, resulting in reduced conductivity, and producing cytotoxicity [36]. Several materials, such as graphene oxide, gold, and polymers, have been proposed as coating materials to minimize the cytotoxicity of AgNWs [37–40]. PDMS-encapsulated AgNWs (AgNWs-PDMS) are promising candidates, and their potential importance has been demonstrated in various applications. However, the use of AgNWs-PDMS as a cell-culture substrate and drug screening platform for measuring cardiomyocyte physiology remains poorly understood [37,40].

Herein, we propose for the first time an AgNWs-E-PDMS hybrid composite cantilever-based drug screening platform for improving cardiomyocyte maturation and evaluating drug-induced cardiotoxicity. The platform provides topographical stimulation and a conductive framework for cell-cell interaction, enhancing cardiomyocyte maturation, as confirmed by WB and RT-qPCR analyses. The proposed platform exhibits excellent cytocompatibility, with cardiomyocyte viability no lower than 95 % compared to the control group. The NRVM and hiPSC-derived cardiomyocytes align along the nanogroove direction and adhere strongly to the substrate, with enhanced electrostatic interactions and improved response to cardiovascular drugs as shown in Fig. 1.

2. Materials and methods

2.1. Materials

Polyurethane acrylate (PUA), polydimethylsiloxane, polyvinyl alcohol (PVA), AgNWs, blebbistatin, E-4031, verapamil, dimethyl

sulfoxide were purchased from Sigma Aldrich, USA and used without any further purification.

2.2. Fabrication of the PVA sacrificial layer

The detailed preparation process of the nanotextured PDMS, the AgNWs surface, and the embedded PDMS cantilever is schematically illustrated in Fig. S1. Firstly, the 800-nm-groove-patterned PUA master mold was fabricated on a glass substrate as described in the supplementary information Fig. S1a [41]. Next, a calculated amount (~80 mg) of PDMS (Base: Curing agent = 10:1) was poured into the PUA mold, and the air bubbles in the PDMS were removed over the course of 30 min in a vacuum desiccator. The PDMS-coated PUA mold was then cured at 80°C for 2 h using a preheated hotplate (Fig. S1b). Afterward, the mold was carefully detached from the PUA mold using a methanol solution (Fig. S1c). Next, 4.5 mL of PVA solution (0.4 g/mL) was poured onto a 4-inch silicon wafer (Fig. S1d). The mold was placed on the PVA, and the desired pressure was applied to transfer the nanopatterns from the PDMS to the water-soluble PVA layer (Fig. S1e). Finally, the PVA layer was completely cured on a hotplate at 115 °C for 12 h, and the nanotextured-PDMS mold was carefully detached from the surface-patterned PVA layer (Fig. S1f).

2.3. Fabrication of PDMS cantilever-based drug screening platform

The fabrication of the AgNWs surface-coated PDMS (AgNWs-S-PDMS) substrate is described in the supplementary information (Fig. S1g–Si). The fabricated nanotextured PDMS, AgNWs-S-PDMS, and AgNWs-E-PDMS substrates were made into a cantilever shape using a roll-to-plate pinnacle die-cutting machine. Next, platinum was deposited at the free end of the cantilever to measure the cantilever displacement using a nanoscale accuracy laser vibrometer. Finally, the PDMS and a glass body were chemically bonded together to form a cantilever device using an O₂ plasma treatment (Femto Science, CUTE-MPR) at 100 W for 60 s. The dimensions of the cantilever were 2 mm in width, 6 mm in length, and 110 μ m in thickness, respectively.

2.4. Statistical analysis

Statistical analyses were performed using Prism GraphPad 9 and the results were expressed as mean \pm standard deviation. The statistical significance of the data was determined by one-way ANOVA followed by Tukey's Honestly Significant Difference test; * p < 0.05 and ** p < 0.01.

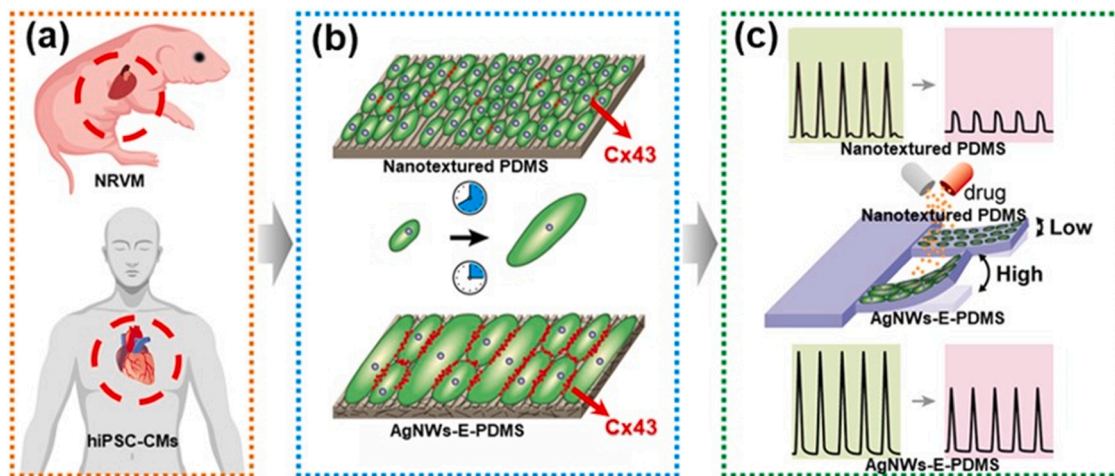


Fig. 1. Conceptual framework of the proposed study. (a) NRVM and hiPSC-derived cardiomyocytes are cultured on a nanotextured PDMS and AgNWs-E-PDMS drug screening platform. (b) The cardiomyocytes align along the groove direction on the nanotextured PDMS and AgNWs-E-PDMS. However, on the AgNWs-E-PDMS, the cardiomyocytes strongly adhere to the substrate due to enhanced electrostatic interactions, leading to greater maturity. (c) The more mature cardiomyocytes cultured on the AgNWs-E-PDMS cantilever responded well to cardiovascular drugs compared with the immature cardiomyocytes.

The rise time and decay time were analyzed and corrected using Fridlericia's formula (corrected duration = absolute duration/(interspike interval)^(1/3)).

3. Results and discussion

3.1. Preliminary characteristics maturation and physiological analysis

The morphology, effects of surface oxidation, wettability, robustness, and mechanical durability of the fabricated cantilevers based on nanotextured PDMS, AgNWs-S-PDMS, and AgNWs-E-PDMS were extensively studied and described in detail in the [supplementary information](#) (Fig. S2–S8). The methods for cell culture and isolation of NRVM are described in the [supplementary information](#). Animal experiments were conducted in compliance with ethical standards approved by the Animal Ethics Committee at Chonnam National University (license number: CNU IACUC-YB-2022–29). NRVM cultured on nanotextured PDMS and AgNWs-E-PDMS cantilevers aligned themselves along the long axis of grooves, while NRVM cultivated on AgNWs-S-PDMS cantilevers adhered less closely to the substrate and showed anisotropic behavior. The exposed nanowires and potential toxicity of the nanotextured PDMS surface limited the ability of the cardiomyocytes to receive topographical stimulation, leading to their anisotropic behavior and low survival rate (Fig. 2a). The cytocompatibility of the cantilever devices was confirmed by analyzing cell growth, proliferation, and viability of cardiomyocytes using a Live/Dead viability/cytotoxicity kit (Cat. No. BDA-1000, Biomax) and confocal laser scanning microscopy on days 1, 3, and 7 of culture (Fig. 2b). The details of the cell viability analysis are described in detail in the [supplementary information](#). The survival rate of NRVM cultured on AgNWs-S-PDMS cantilevers decreased to less than 30 % on day 7, indicating that fully exposed AgNWs can be toxic to cultured cardiomyocytes. However, NRVM cultured on AgNWs-E-PDMS cantilevers maintained a survival rate of more than 95 %, showing similar cytocompatibility to the nanotextured PDMS cantilevers. Therefore, further investigations were only conducted on AgNWs-E-PDMS cantilevers, and the results were compared with those obtained on nanotextured PDMS.

Real-time traces of the cantilever displacement, based on nanotextured PDMS and AgNWs-E-PDMS, resulting from cultured cardiomyocyte contractility were measured using a laser vibrometer on different culture days (Fig. 2c(i, ii)). The details of the contraction force measurement are described in the [supplementary information](#). Cantilever displacement increased with culture time, peaking on day 9, and then decreased due to cardiomyocyte detachment and aggregation [42]. Fig. 2d shows the relative contraction force and beat rate of cardiomyocytes cultured on nanotextured PDMS and AgNWs-E-PDMS cantilevers. The relative contraction force of cultured cardiomyocytes on both cantilevers increased with incubation time until day 9. However, cardiomyocytes cultured on AgNWs-E-PDMS cantilevers exhibited significantly enhanced displacement and relative contraction force compared to those on nanotextured PDMS cantilevers.

Cardiomyocytes cultured on nanotextured PDMS cantilevers survived only for 14 days before senescence caused detachment from the substrate [43]. In contrast, cardiomyocytes cultured on AgNWs-E-PDMS cantilevers survived until day 25 and produced significant cantilever displacement (Fig. 2c(i, ii)). These cells exhibited a longer aging period, higher relative contraction force, and stable beat rate compared to those on the nanotextured PDMS cantilever due to strong cell adhesion, cell-cell interactions, and cardiomyocyte maturation (Fig. 2d(i, ii)). To evaluate improved cell-cell interactions and maturation, immunocytochemical (ICC) staining analysis was performed as described in the [supplementary information](#). The ICC staining analysis of the cardiomyocytes obtained from both types of cantilever devices on day 8 is shown in Fig. 2e(i). The distribution of two important cardiomyocyte proteins (Cx43 and sarcomere length) was more organized and homogeneous around the cell periphery in cardiomyocytes from

AgNWs-E-PDMS cantilevers than those from nanotextured PDMS cantilevers. Sarcomere lengths of cardiomyocytes from nanotextured PDMS and AgNWs-E-PDMS cantilevers were approximately $1.72 \pm 0.04 \mu\text{m}$ and $1.99 \pm 0.02 \mu\text{m}$, respectively (Fig. 2e(ii)). This length influences the generation of contraction force and synchronization by maintaining alignment with parallel myofibrils and neighboring sarcomeres throughout the contraction and relaxation process [44–46]. Cx43 expression, indicative of well-formed intracellular contact, was approximately 1.00 ± 0.05 and 1.44 ± 0.08 in cardiomyocytes from nanotextured and AgNWs-E-PDMS cantilevers, respectively (Fig. 2e(ii)). Enhanced coupling due to increased Cx43 expression improved electrical activity and synchronicity.

3.2. Electrophysiology and protein expression of cardiomyocytes

The influence of a conductive substrate on the electrophysiology and protein expression of cardiomyocytes cultured on nanotextured PDMS and AgNWs-E-PDMS cantilevers was evaluated using calcium (Ca^{2+}) transient, WB, and quantitative RT-qPCR analyses (Fig. 3 and Fig. S9–11, Table S1). After incubation with the Ca^{2+} -sensitive dye Fluo-4 AM for 40 min, cultivated cardiomyocytes were electrically stimulated at 1 Hz until a steady state was achieved. The cardiomyocytes were then excited by an argon laser at 488 nm under a confocal microscope, and the images were recorded for processing and data extraction. Cardiomyocytes from three different regions were selected for Ca^{2+} transient analysis (Fig. 3a, b). On nanotextured PDMS cantilevers, cardiomyocytes exhibited randomly distributed calcium spikes and amplitudes, and their Ca^{2+} transient signals were not fully synchronized with neighboring cardiomyocytes. In contrast, cardiomyocytes on AgNWs-E-PDMS cantilevers displayed coordinated calcium spikes with higher amplitudes and synchronized beating behavior with neighboring cardiomyocytes due to improved electrical cell-cell interaction and maturation, along with higher decay times (Fig. 3c, d) [47,48].

WB and RT-qPCR analysis of cardiomyocytes from both cantilevers confirmed these findings (Fig. 3e). GAPDH protein expression served as an internal control in cardiomyocytes from both cantilevers, and protein markers such as troponin, Cx43, and α -actinin were quantitatively examined through WB analysis, an essential method for evaluating cell maturation and relative protein expression. Cardiomyocytes obtained from AgNWs-E-PDMS cantilevers exhibited significantly increased levels of troponin, Cx43, and α -actinin proteins by 1.56-, 4.59-, and 1.50-times, respectively, compared to those obtained from the nanotextured PDMS cantilever (Fig. 3e). The effect of the AgNWs-E-PDMS cantilever on the expression of troponin, Cx43, α -actinin, NCX, and MYH6 genes in cardiomyocytes was assessed using RT-qPCR analysis. The gene expression of these markers in cardiomyocytes obtained from the AgNWs-E-PDMS cantilever was significantly higher (1.70-, 1.50-, 1.74-, 1.33-, and 1.30- times, respectively) compared to those obtained from the nanotextured PDMS cantilevers (Fig. 3f). The increased protein and gene expression in cardiomyocytes cultivated on AgNWs-E-PDMS cantilever indicate improved maturation and intercellular communication, resulting in enhanced electrophysiology and mechanophysiology.

3.3. Effect of cardiovascular drugs on the cultured cardiomyocytes

The feasibility of nanotextured PDMS and AgNWs-E-PDMS cantilevers was assessed by examining the effect of cardiovascular drugs on the contractility of cardiomyocytes. The investigation was carried out on culture day 8, as the cantilevers maintained stable contractility during the measurement period. DMSO was used to dilute the cardiovascular drugs, and the final DMSO concentration was kept at 0.1 %. The drug concentrations in the culture medium were gradually increased to investigate their effects on the mechanophysiology of cardiomyocytes. The contractility of drug-treated cardiomyocytes was measured after allowing them to stabilize for 15 min. The culture medium was refreshed every 4 h prior to the drug screening procedure.

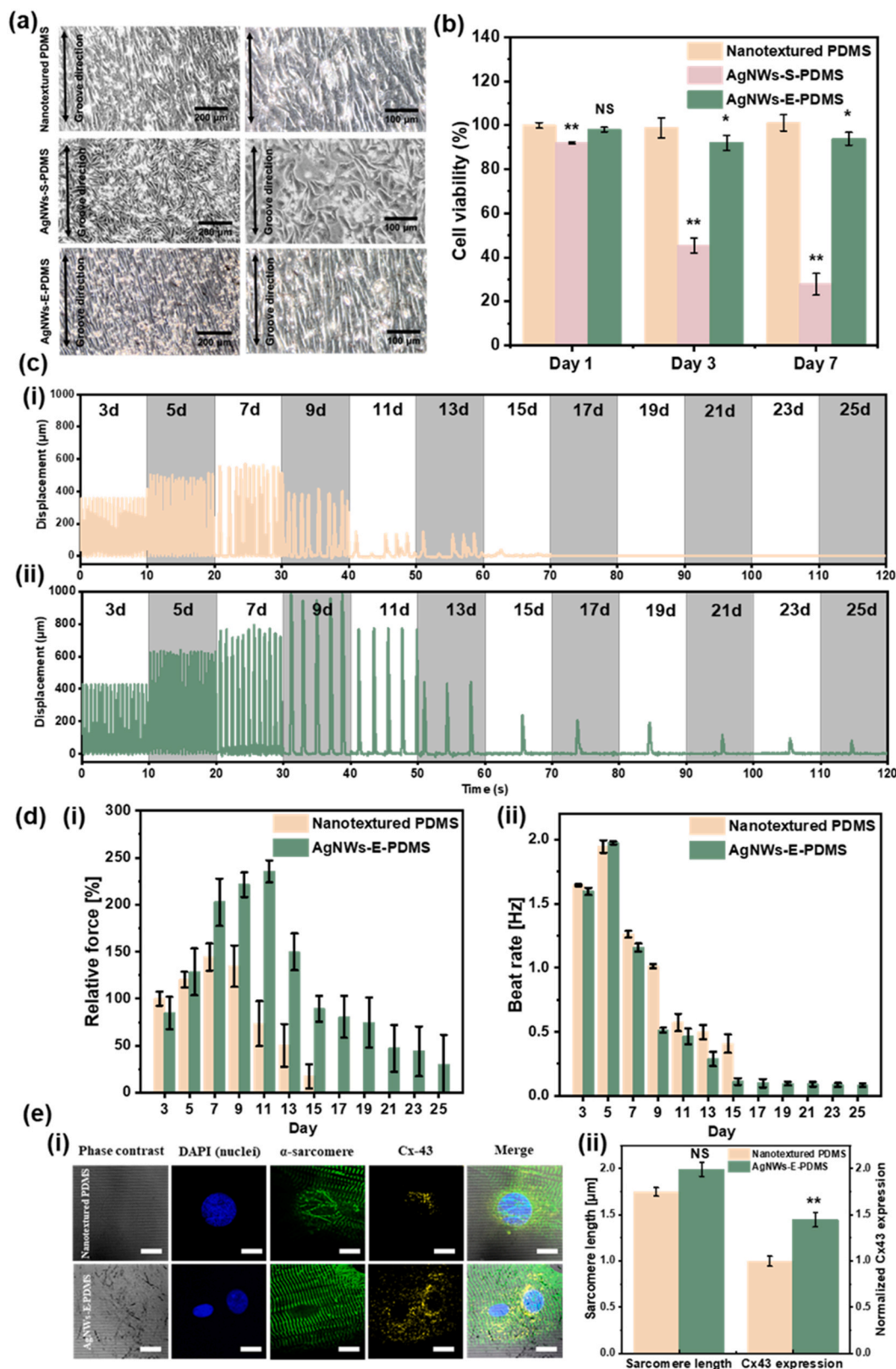


Fig. 2. Cytocompatibility of nanotextured PDMS, AgNWs-S-PDMS, and AgNWs-E-PDMS cantilevers. (a) Cardiomyocytes cultured on these substrates at two different magnifications. (b) Relative cell viability after 1, 3, and 7 days on the substrates. (c) Real-time traces of cantilever displacement caused by cardiomyocyte contraction forces on (i) nanotextured PDMS and (ii) AgNWs-E-PDMS cantilevers on different culture days. (d) Bar plots of relative force and beat rate of the cardiomyocytes cultured on (i) nanotextured PDMS and (ii) AgNWs-E-PDMS cantilevers on different culture days. (e) Immunocytochemical staining images of the cardiomyocytes cultured on the substrates, including optical images, (i) DAPI, α -actinin, and Cx43 expression, and merged images. (ii) Bar plots show α -actinin and Cx43 expression of the cardiomyocytes obtained from the substrates. NS indicates nonsignificant.

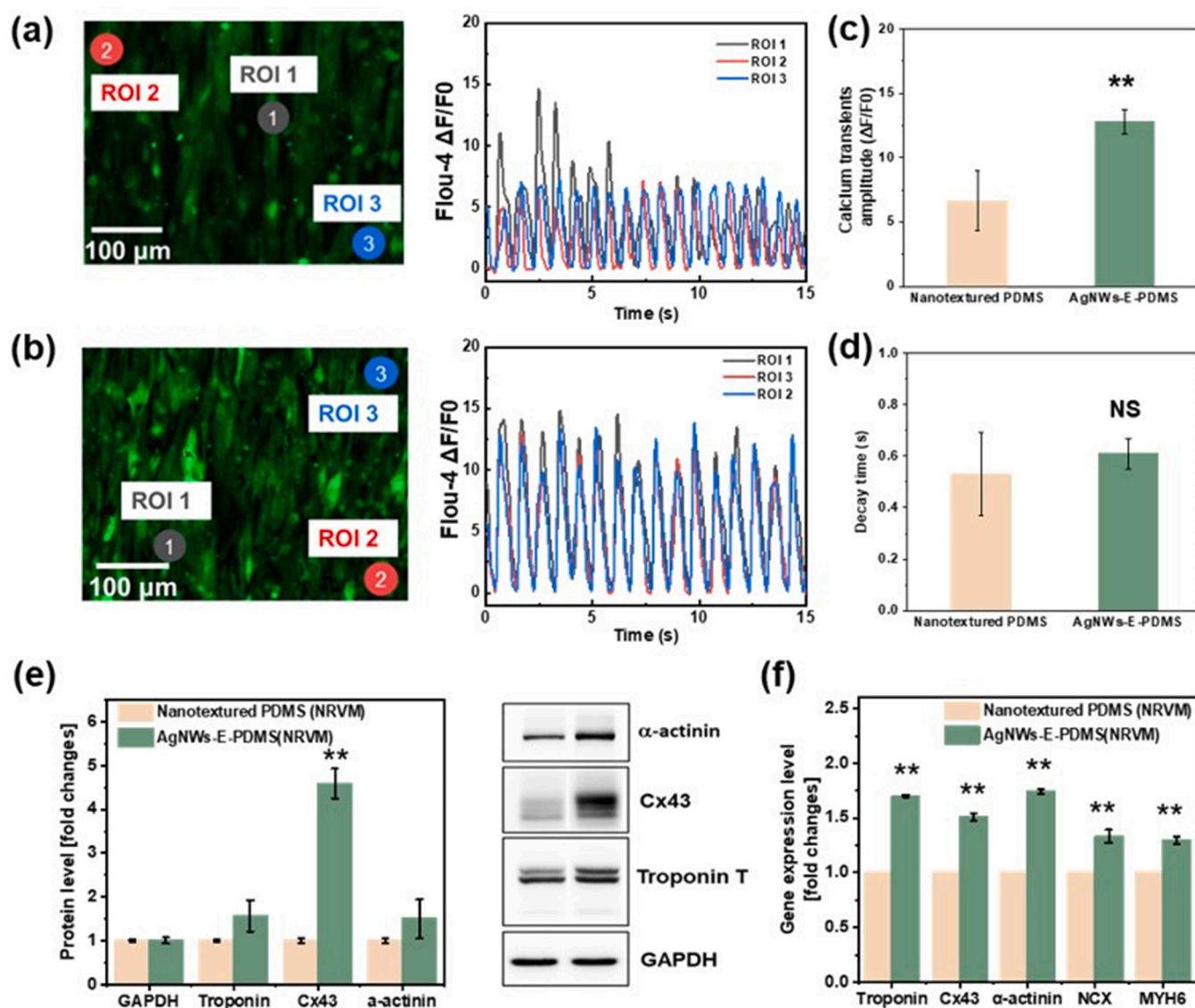


Fig. 3. Electrophysiology and protein expression of cardiomyocytes cultured on nanotextured PDMS and AgNWs-E-PDMS cantilevers. (a, b) Calcium transients of cardiomyocytes cultured on the respective cantilevers, monitored in three independent regions of interest. (c, d) Calcium transients and decay time of the cardiomyocytes obtained from the nanotextured PDMS and AgNWs-E-PDMS cantilevers. (e, f) Western blot and RT-qPCR analyses indicate protein expression levels of the cardiomyocytes on the two cantilevers. NS: Nonsignificant.

Firstly, blebbistatin, an inhibitor of myosin-II-specific ATPase, was utilized to inhibit the contraction of cardiomyocytes. The real-time traces of nanotextured PDMS and AgNWs-E-PDMS cantilevers at varying blebbistatin concentrations were recorded (Fig. 4a). The cantilever displacement was reduced with increasing blebbistatin concentrations on both cantilevers [49]. Even when treated with 1 and 5 μ M blebbistatin, the cardiomyocytes on the AgNWs-E-PDMS cantilevers were able to produce a contraction force, while the cardiomyocytes on the nanotextured PDMS cantilever stopped beating when treated with 500 nM blebbistatin. The relative contraction force of the cardiomyocytes cultured on both cantilevers at varying blebbistatin concentrations was measured (Fig. 4b(i)). It was found that the matured cardiomyocytes on the AgNWs-E-PDMS cantilevers were more drug-resistant than those on the nanotextured PDMS cantilevers. Compared with the control state, the relative contraction force of the cardiomyocytes treated with 500 nM blebbistatin on the nanotextured PDMS and AgNWs-E-PDMS cantilevers decreased by 63 % and 51 %, respectively. Furthermore, the beat rate of the cardiomyocytes on the nanotextured PDMS cantilever and AgNWs-E-PDMS cantilever decreased 2.90- and 0.93-fold

compared with the control state (Fig. 4b(ii)). The rise time and decay time of the cardiomyocytes were defined as the time in which the cardiomyocytes achieve 90 % of their contraction force and the time in which the cardiomyocytes reach 10 % of their contraction force, respectively. Fig. 4b(iii, iv) show the rise time and decay time of the contractility of cardiomyocytes on the nanotextured PDMS and AgNWs-E-PDMS cantilevers. Compared with the control state, the rise time of 500 nM blebbistatin-treated cardiomyocytes on the nanotextured PDMS cantilevers rose 2.21-fold, while the rise time of cardiomyocytes on the AgNWs-E-PDMS cantilever remained unchanged. The decay time of the cardiomyocytes on the nanotextured PDMS and AgNWs-E-PDMS cantilevers was reduced by 1.32- and 0.85-fold, respectively, compared with the control state. This could be due to changes in systolic and diastolic Ca^{2+} values at high blebbistatin concentrations [51]. The cardiomyocytes on both cantilevers showed negative inotropic effects, with an IC_{50} of 92 and 374 nM, respectively (Fig. 4c(i, ii)). A higher IC_{50} indicates a better response from the cardiomyocytes on the AgNWs-E-PDMS cantilever.

Secondly, E-4031, a class III antiarrhythmic drug, was used to induce

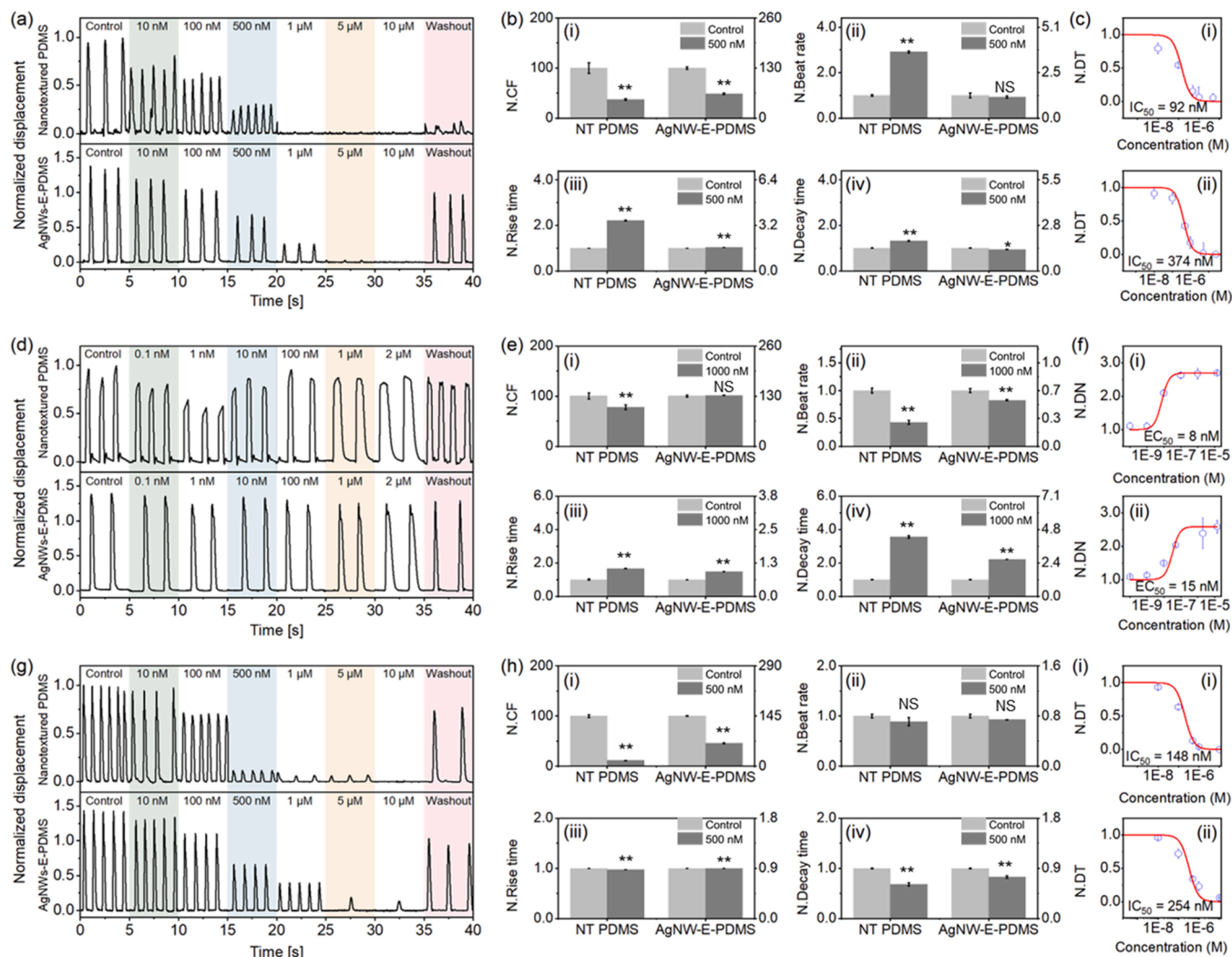


Fig. 4. Effect of cardiovascular drugs on the NRVM cardiomyocytes cultured on nanotextured PDMS and AgNWs-E-PDMS cantilevers. (a), (d), and (g) Real-time traces of cantilever displacement caused by contraction force of cardiomyocytes at different blebbistatin, E-4031, and verapamil concentrations. (b), (e), and (h) Contractile parameters of the blebbistatin, E-4031, and verapamil-treated cardiomyocytes, including contraction force, beat rate, rise time, and decay time. (c), (f), and (i) Drug-dose response curves of the blebbistatin, E-4031, and verapamil on nanotextured PDMS and AgNWs-E-PDMS cantilevers. NS: nonsignificant. N.CF, N.DT, and N.DU denote, normalized contraction force, displacement, and duration, respectively.

cardiotoxicity, and its concentration was increased from 0.1 nM to 2 μM at periodic intervals to measure its effects on the cardiomyocytes cultured on nanotextured PDMS and AgNWs-E-PDMS cantilevers (Fig. 4d). The relative contraction force of cardiomyocytes on AgNWs-E-PDMS cantilevers was largely unaffected by E-4031, even at higher concentrations, while cardiomyocytes on nanotextured PDMS cantilevers showed a decreasing relative contraction force (Fig. 4e(i, ii)). Additionally, a significant change in the beating rate was observed when cardiomyocytes were treated with a higher concentration of E-4031, with the beat rate of the 1 μM-treated cardiomyocytes decreasing 1.28- and 0.99-fold on nanotextured PDMS cantilevers and AgNWs-E-PDMS cantilevers, respectively, compared to the untreated cardiomyocytes (Fig. 4e(iii, iv)). Furthermore, E-4031-treated cardiomyocytes had a concentration-dependent reduction in their rise time on nanotextured PDMS cantilevers, while their rise time increased on AgNWs-E-PDMS cantilevers. The decay duration of cardiomyocyte contractility was prolonged with increasing E-4031 concentration, with the decay duration of 1 μM-treated cardiomyocytes on nanotextured PDMS and AgNWs-E-PDMS cantilevers increasing 3.55- and 2.21-fold, respectively, compared to the control state. The cardiomyocytes cultured on nanotextured PDMS and AgNWs-E-PDMS cantilevers showed a positive

chronotropic effect, with IC_{50} values of 8 and 15 nM, respectively (Fig. 4f(i, ii)).

Thirdly, the effect of verapamil, a class IV phenylalkylamine L-type Ca^{2+} channel blocker, on cultured cardiomyocytes was investigated. Verapamil has been reported to reduce the contraction force of cardiomyocytes, enabling correlation with their toxicity profiles. Cardiomyocytes cultured on nanotextured PDMS and AgNWs-E-PDMS cantilevers were treated with verapamil concentrations ranging from 10 nM to 10 μM at periodic intervals. The real-time traces of the cantilever displacement caused by the contraction force of the verapamil-treated cardiomyocytes at different concentrations were recorded (Fig. 4g). The contraction force of the cardiomyocytes on both cantilevers decreased in a concentration-dependent manner. The beat rate of the 500 nM-treated cardiomyocytes on the nanotextured PDMS cantilever decreased by 1.13-fold compared to the control state, while it remained stable on AgNWs-E-PDMS cantilevers (Fig. 4h(i, ii)). Additionally, increasing verapamil concentrations significantly affected the rise time of the cardiomyocytes, which decreased by 1.14- and 1.08-fold on nanotextured PDMS and AgNWs-E-PDMS cantilevers, respectively, compared to untreated cardiomyocytes. In contrast, the decay time of the cardiomyocytes on both cantilevers decreased with increasing

verapamil concentration (Fig. 4h(iii, iv)). The cardiomyocytes cultured on nanotextured PDMS and AgNWs-E-PDMS cantilevers showed a negative inotropic effect in response to verapamil, with IC₅₀ values of 148 nM and 254 nM, respectively (Fig. 4i(i, ii)).

The advantages of hiPSC-CMs over animal models are significant, as preclinical studies on NRVN have limited predictive accuracy for the human heart. hiPSC-CMs are promising candidates for cell therapy due to their unlimited availability and potential for remuscularization. However, their fetal phenotype in structure and function, including small cell size, absence of T tubules, persistent automaticity, metabolic dependence on glycolysis, and lack of inotropic response to adrenergic stimulation, present challenges for clinical applications and drug testing. To investigate drug responses on immature and mature human cardiomyocytes, hiPSC-CMs were cultured on nanotextured PDMS and AgNWs-E-PDMS cantilevers for drug toxicity screening, as described in the [supplementary information](#). The real-time contractility traces of hiPSC-CMs cultured on these cantilevers showed a concentration-dependent reduction in relative contraction force with increasing blebbistatin concentration. The AgNWs-E-PDMS cantilever exhibited a significantly higher relative displacement than the nanotextured PDMS cantilever, with hiPSC-CMs on the former able to cause displacement even at higher blebbistatin concentrations. Moreover, the AgNWs-E-

PDMS cantilever retained 75 % of its displacement after washing the hiPSC-CMs with a plating medium, and the beating frequency of the hiPSC-CMs returned to initial values, whereas the nanotextured PDMS cantilever stopped responding to the drug and did not produce any displacement (Fig. 5a).

Fig. 5b(i) shows that increasing the concentration of blebbistatin reduced the relative contraction force of hiPSC-CMs cultured on nanotextured PDMS and AgNWs-E-PDMS cantilevers. The relative contraction force of hiPSC-CMs treated with 500 nM blebbistatin on nanotextured PDMS and AgNWs-E-PDMS cantilevers decreased by 3.13- and 2.02-fold, respectively, compared to untreated hiPSC-CMs. Fig. 5b(ii) demonstrating that the beating rate of hiPSC-CMs treated with 500 nM blebbistatin on nanotextured PDMS cantilevers decreased by approximately 1.72-fold compared to the control state, while the beating rate on AgNWs-E-PDMS cantilevers remained comparable to the control state. Fig. 5b(iii) indicates that hiPSC-CMs treated with 500 nM blebbistatin on AgNWs-E-PDMS cantilevers exhibited no statistically significant variations in the rise time, while an increasing trend was observed on nanotextured PDMS cantilevers. Additionally, the decay time of hiPSC-CMs treated with 500 nM blebbistatin on nanotextured PDMS cantilevers was enhanced by 1.32-fold compared to the control state, with no significant changes observed in hiPSC-CMs on AgNWs-E-

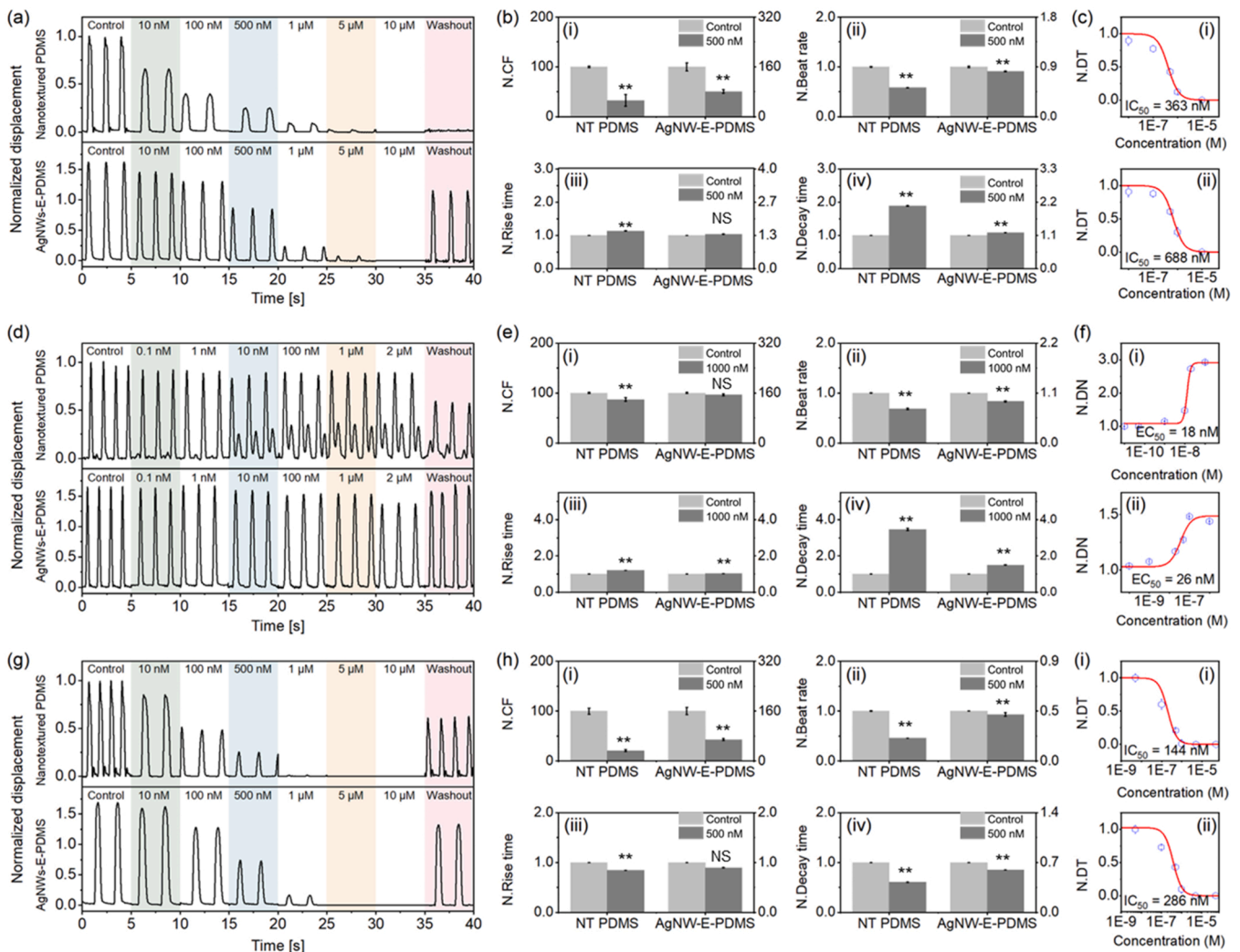


Fig. 5. Effect of cardiovascular drugs on the hiPSC cultured on nanotextured PDMS and AgNWs-E-PDMS cantilevers. (a), (d), and (g) Real-time traces of cantilever displacement caused by contraction force of hiPSC at different blebbistatin, E-4031, and verapamil concentrations. (b), (e), and (h) Contractile parameters of the blebbistatin, E-4031, and verapamil-treated hiPSC, including contraction force, beat rate, rise time, and decay time. (c), (f), and (i) Drug-dose response curves of the blebbistatin, E-4031, and verapamil on nanotextured PDMS and AgNWs-E-PDMS cantilevers. NS: nonsignificant. N.C.F, N.D.T, and N.D.U denote, normalized contraction force, displacement, and duration, respectively.

PDMS cantilevers (Fig. 5b(iv)). The drug-dose response curve exhibited negative inotropic effects for hiPSC-CMs on both cantilevers, with IC₅₀ values of 363 and 688 nM for nanotextured PDMS and AgNWs-E-PDMS cantilevers, respectively (Fig. 5c(i, ii)).

The influence of E-4031 on the contractile properties of hiPSC-CMs on nanotextured PDMS and AgNWs-E-PDMS cantilevers was assessed at varying concentrations (Fig. 5d) [50]. On nanotextured PDMS cantilevers, hiPSC-CMs produced a second beat at a drug concentration of 10 nM, and irregular beating rates resulted from membrane potential disturbances. E-4031 caused repolarization delay, allowing for Ca²⁺ ion re-entry and incomplete depolarization, leading to early after-depolarizations (EADs) during cardiac action potential repolarization and resulting in disturbances in intracellular calcium dynamics and arrhythmic cell beating [51,52]. In contrast, hiPSC-CMs on AgNWs-E-PDMS cantilevers maintained stable beating despite high E-4031 concentrations, while the relative contraction force of hiPSC-CMs on both cantilevers was unaffected by increasing the drug concentration (Fig. 5e(i)). E-4031 decreased the beating rate of hiPSC-CMs, more prominently on nanotextured PDMS cantilevers due to prolonged repolarization time [53]. At 1 μM E-4031, the beating rate of hiPSC-CMs on nanotextured PDMS and AgNWs-E-PDMS cantilevers decreased by 1.49- and 1.20-fold, respectively, compared to the control (Fig. 5e(ii)). The rise time of hiPSC-CMs significantly increased on both cantilevers with increasing E-4031 concentration. The rise time of 1 μM E-4031-treated hiPSC-CMs on nanotextured PDMS and AgNWs-E-PDMS cantilevers increased by 1.19- and 1.03-fold, respectively, compared to untreated hiPSC-CMs (Fig. 5e(iii)). Moreover, a significant increase was observed in the decay time of hiPSC-CMs on both cantilevers, rising by 3.45- and 1.50-fold on nanotextured PDMS and AgNWs-E-PDMS cantilevers, respectively, compared to the control state (Fig. 5e(iv)). This may be attributed to the blocking of the hERG channel by E-4031, causing significant delays in action potential repolarization [54]. Fig. 5f(i, ii) shows the positive chronotropic effects of hiPSC-CMs on both cantilevers, with EC₅₀ values of 18 and 26 nM for nanotextured PDMS and AgNWs-E-PDMS cantilevers, respectively.

The hiPSC-CMs on the nanotextured PDMS and AgNWs-E-PDMS cantilevers were treated at periodic intervals with different verapamil concentrations ranging from 10 nM to 10 μM. The real-time traces of the nanotextured PDMS and AgNWs-E-PDMS cantilever displacement caused by the contraction force of the verapamil-treated hiPSC-CMs at different concentrations are shown in Fig. 5g. Verapamil indirectly alters contractility by blocking the voltage-dependent calcium channels and showing a drug-induced effect on beat rate and duration, particularly at high concentrations [55]. Verapamil reduces the influx of Ca²⁺ ions, which leads to decreases in both the beating rate and contractility [56]. A larger number of free Ca²⁺ ions were prevented from entering the cells, meaning that less calcium would be released from the intracellular calcium sources. Increasing the verapamil concentration not only decreases the contraction force and beat rate but also the rise time and decay time of the hiPSC-CMs [57,58]. The hiPSC-CMs cultured on both cantilevers showed a reduced force and beat rate, and eventually stopped beating at high verapamil concentrations. The relative contraction force and beat rate of the 500 nM-treated hiPSC-CMs on the nanotextured PDMS cantilever decreased sharply 4.79- and 2.18-fold, respectively compared with the control state, whereas the hiPSC-CMs on the AgNWs-E-PDMS cantilever decreased 2.33- and 1.07-fold, respectively, compared with the control state at the same concentration (Fig. 5h(i, ii)). The rise time of the 500 nM-treated hiPSC-CMs on the nanotextured PDMS and AgNWs-E-PDMS cantilevers increased 1.18- and 1.12-fold, respectively, compared with the untreated hiPSC-CMs (Fig. 5h(iii)). The decay time of the 500 nM-treated hiPSC-CMs on the nanotextured PDMS and AgNWs-E-PDMS cantilevers increased 1.65- and 1.17-fold, respectively, compared with the control state (Fig. 5h(iv)). The hiPSC-CMs cultured on the nanotextured PDMS and AgNWs-E-PDMS cantilevers showed a negative inotropic effect, with IC₅₀ values of 144 and 286 nM, respectively (Fig. 5i(i, ii)).

RT-qPCR analysis was performed on the cardiomyocytes obtained from nanotextured PDMS and AgNWs-E-PDMS cantilevers, both before and after drug testing, to investigate the high level of cell resistance and drug endurance observed in the cardiomyocytes (Fig. 6a, b). The expression of Cx43, troponin T, and alpha-actinin in cardiomyocytes was assessed before and after drug treatment. Treatment with blebbistatin, E-4031, and verapamil resulted in a decrease in Cx43 expression in cardiomyocytes cultured on nanotextured PDMS cantilevers by 1.23-, 1.48-, and 1.23-fold, respectively, compared to the control state. The Cx43 expression in cardiomyocytes cultured on AgNWs-E-PDMS cantilevers also decreased, albeit to a lesser extent (1.02-, 1.19-, and 1.12-fold) following treatment with blebbistatin, E-4031, and verapamil, respectively. Similarly, the troponin expression in cardiomyocytes on nanotextured PDMS and AgNWs-E-PDMS cantilevers decreased by 1.39-, 1.06-, and 1.28-fold and 1.16-, 1.02-, and 1.22-fold, respectively, following treatment with blebbistatin, E-4031, and verapamil. RT-qPCR analysis revealed that cardiomyocytes cultured on AgNWs-E-PDMS cantilevers exhibited greater resistance and endurance to the tested cardiovascular drugs than immature cardiomyocytes cultured on nanotextured PDMS cantilevers.

There were similarities and differences observed in the drug response between NRVM and hiPSC-CMs cultured on the AgNWs-E-PDMS cantilever (Fig. S12). The beating frequency of NRVM decreased with increasing blebbistatin concentration, while the beating frequency of hiPSC-CMs decreased to a lesser extent. Although there were no statistically significant differences in the relative contraction forces of blebbistatin-treated NRVM and hiPSC-CMs, hiPSC-CMs performed slightly better (Fig. S12a, b). The beating frequency of 1 μM E-4031-treated NRVM and hiPSC-CMs decreased by 1.41- and 1.20-fold, respectively, compared to untreated cardiomyocytes. However, no significant differences in the relative contractile forces of the two cell types were found (Fig. S12c, d). For all concentrations of verapamil, the beating frequency of NRVM and hiPSC-CMs exhibited a similar trend, although the relative contraction force of both cell types treated with 500 nM verapamil decreased compared to untreated cells (Fig. S12e, f). Our findings demonstrate that hiPSC-CMs are more resistant to the tested cardiovascular drugs, exhibit greater endurance, and are more sensitive to drugs than NRVM, highlighting the distinct species-specificities of the two cell types. Further research is required to better understand their unique biological characteristics.

4. Conclusion

In this study, we proposed the AgNWs-E-PDMS cantilever to improve cardiomyocyte maturation and analysis of drug-induced cardiotoxicity. The PDMS protection layer efficiently protects AgNWs from oxidation, thereby significantly reducing cytotoxicity. The conductive framework beneath the nanotextured PDMS provides better cell-to-cell connectivity. The simultaneous application of topographical stimulation and the conductive framework improves cell maturation. The cardiomyocytes cultured on the AgNWs-E-PDMS cantilever did not decrease to less than 95 % relative to the control cardiomyocytes, signifying the excellent cytocompatibility of the AgNWs-E-PDMS. The improved cell-cell interactions and maturation of the cardiomyocytes were confirmed by WB and RT-qPCR analyses. The protein and gene expression of the cardiomyocytes cultured on the AgNWs-E-PDMS cantilever were enhanced by 4.59- and 1.75-fold, respectively, compared to the control cardiomyocytes. Finally, the cardiomyocytes cultured on the nanotextured PDMS and AgNWs-E-PDMS cantilevers were exposed to various cardiovascular drugs to evaluate drug-induced cardiotoxicity. The matured cardiomyocytes cultured on the AgNWs-E-PDMS exhibited higher IC₅₀ values, indicating greater resistance to cardiovascular drugs. We believe that the proposed AgNWs-E-PDMS cantilever has promising potential in drug screening and tissue engineering applications.

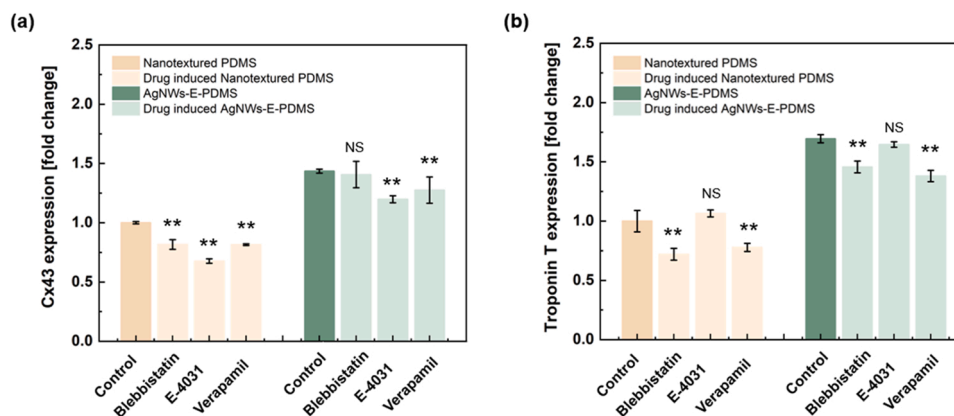


Fig. 6. (a, b) RT-qPCR analysis revealed the expression levels of various proteins on the nanotextured PDMS and AgNWs-E-PDMS cantilever both before and after the drug testing. NS represent non-significant.

CRedit authorship contribution statement

Yuyan Liu: Conceptualization, Investigation, Validation, Formal analysis, Data curation, Visualization, Writing – original draft. **Nomin-Erdene Oyunbaatar:** Participated in cardiomyocytes experiment, Data curation, Formal analysis, Investigation, Methodology, Visualization, Writing - review & editing. **Arunkumar Shanmugasundaram:** Investigation, Validation, Formal analysis, Writing – original draft, Writing – review & editing. **Eung-Sam Kim:** Methodology, Formal analysis. **Bong-Kee Lee:** Methodology, Formal analysis. **Dong-Weon Lee:** Supervision, Funding acquisition, Conceptualization, Writing – review & editing.

Declaration of Competing Interest

The authors declare that they have no known competing financial interests or personal relationships that could have appeared to influence the work reported in this paper.

Data Availability

Data will be made available on request.

Acknowledgements

This study was supported by a National Research Foundation of Korea (NRF) grant funded by the Korean Government (MSIT) (No. 2020R1A5A8018367 and RS-2022-00165505). The authors express their sincere gratitude for the invaluable help and support provided by Dr. Minam Lee during the RT-qPCR investigation.

Appendix A. Supporting information

Supplementary data associated with this article can be found in the online version at [doi:10.1016/j.snb.2023.134014](https://doi.org/10.1016/j.snb.2023.134014).

References

- [1] S.S. Virani, A. Alonso, E.J. Benjamin, M.S. Bittencourt, C.W. Callaway, A.P. Carson, A.M. Chamberlain, A.R. Chang, S. Cheng, F.N. Delling, L. Djousse, Heart disease and stroke statistics—2020 update: a report from the American heart association, *Circulation* 141 (2020) 139–596, <https://doi.org/10.1161/CIR.0000000000000757>.
- [2] S.D. Wiviott, E. Braunwald, C.H. McCabe, G. Montalescot, W. Ruzyllo, S. Gottlieb, F.J. Neumann, D. Ardissino, S. De Servi, S.A. Murphy, J. Riesmeyer, Prasugrel versus clopidogrel in patients with acute coronary syndromes, *N. Engl. J. Med.* 357 (2007) 2001–2015, <https://doi.org/10.1056/NEJMoa0706482>.
- [3] L. Wallentin, R.C. Becker, A. Budaj, C.P. Cannon, H. Emanuelsson, C. Held, J. Horrow, S. Husted, S. James, H. Katus, K.W. Mahaffey, Ticagrelor versus clopidogrel in patients with acute coronary syndromes, *N. Engl. J. Med.* 361 (2009) 1045–1057, <https://doi.org/10.1056/NEJMoa0904327>.
- [4] A. Mathur, P. Loskill, S. Hong, J.Y. Lee, S.G. Marcus, L. Dumont, B.R. Conklin, H. Willenbring, L.P. Lee, K.E. Healy, Human induced pluripotent stem cell-based microphysiological tissue models of myocardium and liver for drug development, *Stem Cell Res. Ther.* 4 (2013) 1–5, <https://doi.org/10.1186/scrt375>.
- [5] M. Hay, D.W. Thomas, J.L. Craighead, C. Economides, J. Rosenthal, Clinical development success rates for investigational drugs, *Nat. Biotechnol.* 32 (2014) 40–51, <https://doi.org/10.1038/nbt.2786>.
- [6] T. Takebe, R. Imai, S. Ono, The current status of drug discovery and development as originated in united states academia: the influence of industrial and academic collaboration on drug discovery and development, *Clin. Transl. Sci.* 11 (2018) 597–606, <https://doi.org/10.1111/cts.12577>.
- [7] E. Karbassi, A. Fenix, S. Marchiano, N. Muraoka, K. Nakamura, X. Yang, C. E. Murry, Cardiomyocyte maturation: advances in knowledge and implications for regenerative medicine, *Nat. Rev. Cardiol.* 17 (2020) 341–359, <https://doi.org/10.1038/s41569-019-0331-x>.
- [8] F.B. Bedada, M. Wheelwright, J.M. Metzger, Maturation status of sarcomere structure and function in human iPSC-derived cardiac myocytes, *Biochim. Biophys. Acta Mol. Cell Res.* 2016 (1863) 1829–1838, <https://doi.org/10.1016/j.bbamcr.2015.11.005>.
- [9] P.P. Abadi, J.C. Garbern, S. Behzadi, M.J. Hill, J.S. Tresback, T. Heydari, M. R. Ejtehadi, N. Ahmed, E. Copley, H. Aghaverdi, R.T. Lee, Engineering of mature human induced pluripotent stem cell-derived cardiomyocytes using substrates with multiscale topography, *Adv. Funct. Mater.* 28 (2018), 1707378, <https://doi.org/10.1002/adfm.201707378>.
- [10] J.L. Ruan, N.L. Tulloch, M.V. Razumova, M. Saiget, V. Muskheli, L. Pabon, H. Reinecke, M. Regnier, C.E. Murry, Mechanical stress conditioning and electrical stimulation promote contractility and force maturation of induced pluripotent stem cell-derived human cardiac tissue, *Circulation* 134 (2016) 1557–1567, <https://doi.org/10.1161/CIRCULATIONAHA.114.014998>.
- [11] R.E. Ahmed, T. Anzai, N. Chanthra, H. Uosaki, A brief review of current maturation methods for human induced pluripotent stem cells-derived cardiomyocytes, *Cell. Dev. Biol.* 8 (2020) 178, <https://doi.org/10.3389/fcell.2020.00178>.
- [12] Y. Guo, W.T. Pu, Cardiomyocyte maturation: new phase in development, *Circ. Res.* 126 (2020) 1086–1106, <https://doi.org/10.1161/CIRCRESAHA.119.315862>.
- [13] R.R. Besser, M. Ishahak, V. Mayo, D. Carbonero, I. Claure, A. Agarwal, Engineered microenvironments for maturation of stem cell derived cardiac myocytes, *Theranostics* 18 (2018) 124, <https://doi.org/10.7150/thno.19441>.
- [14] V. Hosseini, S. Gantenbein, I. Avalos Vizcarra, I. Schoen, V. Vogel, Stretchable silver nanowire microelectrodes for combined mechanical and electrical stimulation of cells, *Adv. Healthc. Mater.* 5 (2016) 2045–2054, <https://doi.org/10.1002/adhm.201600045>.
- [15] A.M. Gerdes, S.E. Kellerman, J.A. Moore, K.E. Muffly, L.C. Clark, P.Y. Reaves, K. B. Malec, P.P. McKeown, D.D. Schocken, Structural remodeling of cardiac myocytes in patients with ischemic cardiomyopathy, *Circulation* 86 (1992) 426–430, <https://doi.org/10.1161/01.cir.86.2.426>.
- [16] D. Carson, M. Hnilova, X. Yang, C.L. Nemeth, J.H. Tsui, A.S. Smith, A. Jiao, M. Regnier, C.E. Murry, C. Tamerler, D.H. Kim, Nanotopography-induced structural anisotropy and sarcomere development in human cardiomyocytes derived from induced pluripotent stem cells, *ACS Appl. Mater. Interfaces* 8 (2016) 21923–21932, <https://doi.org/10.1021/acsami.5b11671>.
- [17] T. Dvir, B.P. Timko, M.D. Brigham, S.R. Naik, S.S. Karajanagi, O. Levy, H. Jin, K. K. Parker, R. Langer, D.S. Kohane, Nanowired three-dimensional cardiac patches, *Nat. Nanotechnol.* 6 (2011) 720–725, <https://doi.org/10.1038/nnano.2011.160>.
- [18] H.S. Yang, B. Lee, J.H. Tsui, J. Macadangang, S.Y. Jang, S.G. Im, D.H. Kim, Electroconductive nanopatterned substrates for enhanced myogenic differentiation and maturation, *Adv. Healthc. Mater.* 5 (2018) 137–145, <https://doi.org/10.1002/adhm.201500003>.
- [19] Y.J. Jeong, D.S. Kim, J.Y. Kim, N.E. Oyunbaatar, A. Shanmugasundaram, E.S. Kim, D.W. Lee, On-stage bioreactor platform integrated with nano-patterned and gold-coated pdms diaphragm for live cell stimulation and imaging, *Mater. Sci. Eng. C* 118 (2021), 111355, <https://doi.org/10.1016/j.msec.2020.111355>.

- [20] J. Kim, A. Shanmugasundaram, D.W. Lee, Enhancement of cardiac contractility using gold-coated su-8 cantilevers and their application to drug-induced cardiac toxicity tests, *Analyst* 146 (2012) 6768–6779, <https://doi.org/10.1039/D1AN01337H>.
- [21] H.J. Cho, H.J. Lee, Y.J. Chung, J.Y. Kim, H.J. Cho, H.M. Yang, Y.W. Kwon, H. Y. Lee, B.H. Oh, Y.B. Park, H.S. Kim, Generation of human secondary cardiospheres as a potent cell processing strategy for cell-based cardiac repair, *Biomaterials* 34 (2013) 651–661, <https://doi.org/10.1016/j.biomaterials.2012.10.011>.
- [22] B. Peña, V. Martinelli, M. Jeong, S. Bosi, R. Lapasin, M.R. Taylor, C.S. Long, R. Shandas, D. Park, L. Mestroni, Biomimetic polymers for cardiac tissue engineering, *Biomacromolecules* 17 (2016) 1593–1601, <https://doi.org/10.1021/acs.biomac.5b01734>.
- [23] D. Fischer, Y. Li, B. Ahlemeyer, J. Kriegelstein, T. Kissel, In vitro cytotoxicity testing of polycations: influence of polymer structure on cell viability and hemolysis, *Biomaterials* 24 (2003) 1121–1131, [https://doi.org/10.1016/S0142-9612\(02\)00445-3](https://doi.org/10.1016/S0142-9612(02)00445-3).
- [24] S. Choi, S.I. Han, D. Jung, H.J. Hwang, C. Lim, S. Bae, O.K. Park, C.M. Tschabrunn, M. Lee, S.Y. Bae, J.W. Yu, Highly conductive, stretchable and biocompatible ag–au core–sheath nanowire composite for wearable and implantable bioelectronics, *Nat. Nanotechnol.* 13 (2018) 1048–1056, <https://doi.org/10.1038/s41565-018-0226-8>.
- [25] G. Kaur, R. Adhikari, P. Cass, M. Bown, P. Gunatillake, electrically conductive polymers and composites for biomedical applications, *RSC Adv.* 5 (2015) 37553–37567, <https://doi.org/10.1039/C5RA01851J>.
- [26] M. Yang, Z.D. Hood, X. Yang, M. Chi, Y. Xia, Facile synthesis of Ag@ Au core–sheath nanowires with greatly improved stability against oxidation, *Chem. Commun.* 53 (2017) 1965–1968.
- [27] S. Ye, A.R. Rathmell, Z. Chen, I.E. Stewart, B.J. Wiley, Metal nanowire networks: the next generation of transparent conductors, *Adv. Mater.* 26 (2016) 6670–6687, <https://doi.org/10.1002/adma.201402710>.
- [28] L. Hu, H.S. Kim, J.Y. Lee, P. Peumans, Y. Cui, Scalable coating and properties of transparent, flexible, silver nanowire electrodes, *ACS Nano* 4 (2010) 2955–2963, <https://doi.org/10.1021/nn1005232>.
- [29] Y. Tan, D. Richards, R. Xu, S. Stewart-Clark, S.K. Mani, T.K. Borg, D.R. Menick, B. Tian, Y. Mei, Silicon nanowire-induced maturation of cardiomyocytes derived from human induced pluripotent stem cells, *Nano Lett.* 15 (2015) 2765–2772, <https://doi.org/10.1021/nl502227a>.
- [30] A.S. Smith, H. Yoo, H. Yi, E.H. Ahn, J.H. Lee, G. Shao, E. Nagornyak, M. A. Laflamme, C.E. Murry, D.H. Kim, Micro- and nano-patterned conductive graphene-peg hybrid scaffolds for cardiac tissue engineering, *Chem. Commun.* 53 (2017) 7412–7415, <https://doi.org/10.1039/C7CC01988B>.
- [31] V. Martinelli, S. Bosi, B. Peña, G. Baj, C.S. Long, O. Sbaizero, M. Giacca, M. Prato, L. Mestroni, L. 3D Carbon-nanotube-based composites for cardiac tissue engineering, *ACS Appl. Biol. Mater.* 1 (2018) 1530–1537, <https://doi.org/10.1021/acsbam.8b00440>.
- [32] X.P. Li, K.Y. Qu, B. Zhou, F. Zhang, Y.Y. Wang, O.D. Abodunrin, Z. Zhu, N. P. Huang, Electrical stimulation of neonatal rat cardiomyocytes using conductive polydopamine-reduced graphene oxide-hybrid hydrogels for constructing cardiac microtissues, *Colloids Surf. B* 205 (2021), 111844, <https://doi.org/10.1016/j.colsurfb.2021.111844>.
- [33] S.R. Shin, S.M. Jung, M. Zalabany, K. Kim, P. Zorlutuna, S.B. Kim, M. Nikkha, M. Khabiri, M. Azize, J. Kong, K.T. Wan, Carbon-nanotube-embedded hydrogel sheets for engineering cardiac constructs and bioactuators, *ACS Nano* 7 (2013) 2369–2380, <https://doi.org/10.1021/nn305559j>.
- [34] J. Kim, J. Lee, H.N. Kim, P. Kang, J. Choi, M.F. Haque, D. Kang, S. Nam, Uniaxially crumpled graphene as a platform for guided myotube formation, *Microsyst. Nanoeng.* 5 (2019) 1–10, <https://doi.org/10.1038/s41378-019-0098-6>.
- [35] A. Navaei, H. Saini, W. Christenson, R.T. Sullivan, R. Ros, M. Nikkha, Gold nanorod-incorporated gelatin-based conductive hydrogels for engineering cardiac tissue constructs, *Acta Biomater.* 41 (2016) 133–146, <https://doi.org/10.1016/j.actbio.2016.05.027>.
- [36] Y. Han, R. Lupitsky, T.M. Chou, C.M. Stafford, H. Du, S. Sukhishvili, Effect of oxidation on surface-enhanced raman scattering activity of silver nanoparticles: a quantitative correlation, *Anal. Chem.* 83 (2011) 5873–5880, <https://doi.org/10.1021/ac2005839>.
- [37] W.H. Chae, T. Sanniccolo, J.C. Grossman, Double-sided graphene oxide encapsulated silver nanowire transparent electrode with improved chemical and electrical stability, *ACS Appl. Mater. Interface* 12 (2020) 17909–17920, <https://doi.org/10.1021/acsami.0c03587>.
- [38] B.Y. Wang, E.S. Lee, Y.J. Oh, H.W. Kang, A silver nanowire mesh overcoated protection layer with graphene oxide as a transparent electrode for flexible organic solar cells, *RSC Adv.* 7 (2017) 52914–52922, <https://doi.org/10.1039/C7RA10889C>.
- [39] A. Wickham, M. Vagin, H. Khalaf, S. Bertazzo, P. Hodder, S. Dänmark, T. Bengtsson, J. Altamiras, D. Ali, Electroactive biomimetic collagen-silver nanowire composite scaffolds, *Nanoscale* 8 (2016) 14146–14155, <https://doi.org/10.1039/C6NR02027E>.
- [40] S. Jiang, C.P. Teng, Fabrication of silver nanowires-loaded polydimethylsiloxane film with antimicrobial activities and cell compatibility, *Mater. Sci. Eng.: C* 70 (2017) 1011–1017, <https://doi.org/10.1016/j.msec.2016.04.094>.
- [41] D.S. Kim, Y.J. Jeong, A. Shanmugasundaram, N.E. Oyunbaatar, J. Park, E.S. Kim, B. K. Lee, D.W. Lee, 64 Pt/PDMS hybrid cantilever arrays with an integrated strain sensor for a high-throughput drug toxicity screening application, *Biosens. Bioelectron.* 190 (2021), 113380, <https://doi.org/10.1016/j.bios.2021.113380>.
- [42] D.S. Kim, Y.W. Choi, A. Shanmugasundaram, Y.J. Jeong, J. Park, N.E. Oyunbaatar, E.S. Kim, M. Choi, D.W. Lee, Highly durable crack sensor integrated with silicone rubber cantilever for measuring cardiac contractility, *Nat. Comm.* 11 (2020) 1–13, <https://doi.org/10.1038/s41467-019-14019-y>.
- [43] D.S. Kim, Y.J. Jeong, B.K. Lee, A. Shanmugasundaram, D.W. Lee, Piezoresistive sensor-integrated pdms cantilever: a new class of device for measuring the drug-induced changes in the mechanical activity of cardiomyocytes, *Sens. Actuators B: Chem.* 240 (2017) 566–572, <https://doi.org/10.1016/j.snb.2016.08.167>.
- [44] J.G. Jacot, A.D. McCulloch, J.H. Omens, Substrate stiffness affects the functional maturation of neonatal rat ventricular myocytes, *Biophys. J.* 95 (2008) 3479–3487, <https://doi.org/10.1529/biophysj.107.124545>.
- [45] V. Sequeira, L.L. Nijenkamp, J.A. Regan, J. van der Velden, The physiological role of cardiac cytoskeleton and its alterations in heart failure, *Biochim Biophys. Acta Biomembr.* BBA-BIOMEMBRANES 2014 (1838) 700–722, <https://doi.org/10.1016/j.bbamem.2013.07.011>.
- [46] N.E. Oyunbaatar, A. Shanmugasundaram, Y.J. Jeong, B.K. Lee, E.S. Kim, D.W. Lee, Micro-patterned SU-8 cantilever integrated with metal electrode for enhanced electromechanical stimulation of cardiac cells, *Colloids Surf. B* 186 (2020), 110682, <https://doi.org/10.1016/j.colsurfb.2019.110682>.
- [47] C. Zhu, A.E. Rodda, V.X. Truong, Y. Shi, K. Zhou, J.M. Haynes, B. Wang, W. D. Cook, J.S. Forsythe, Increased cardiomyocyte alignment and intracellular calcium transients using micropatterned and drug-releasing poly (glycerol sebacate) elastomers, *ACS Biomater. Sci. Eng.* 4 (2018) 2494–2504, <https://doi.org/10.1021/acsbomaterials.8b00084>.
- [48] M. Miragoli, J.L. Sanchez-Alonso, A. Bhargava, P.T. Wright, M. Sikkil, S. Schobesberger, I. Diakonov, P. Novak, A. Castaldi, P. Cattaneo, A.R. Lyon, Microtubule-dependent mitochondria alignment regulates calcium release in response to nanomechanical stimulus in heart myocytes, *Cell Rep.* 14 (2016) 140–151, <https://doi.org/10.1016/j.celrep.2015.12.014>.
- [49] W. Li, X. Luo, Y. Ulbricht, K. Guan, Blebbistatin Protects iPSC-CMs from hypercontraction and facilitates automated patch-clamp based electrophysiological, study, *Stem Cell Res.* 56 (2021), 102565, <https://doi.org/10.1016/j.scr.2021.102565>.
- [50] S. Peng, A.E. Lacerda, G.E. Kirsch, A.M. Brown, A. Bruening-Wright, The action potential and comparative pharmacology of stem cell-derived human cardiomyocytes, *J. Pharmacol. Toxicol. Methods* 61 (2010) 277–286, <https://doi.org/10.1016/j.jvasc.2010.01.014>.
- [51] T. Hayakawa, T. Kunihiro, T. Ando, S. Kobayashi, E. Matsui, H. Yada, Y. Kanda, J. Kurokawa, T. Furukawa, Image-based evaluation of contraction-relaxation kinetics of human-induced pluripotent stem cell-derived cardiomyocytes: correlation and complementarity with extracellular electrophysiology, *J. Mol. Cell. Cardiol.* 77 (2014) 178–191, <https://doi.org/10.1016/j.yjmcc.2014.09.010>.
- [52] X. Zhang, L. Guo, H. Zeng, S.L. White, M. Furniss, B. Balasubramanian, E. Lis, A. Lagrutta, F. Sannajust, L.L. Zhao, B. Xi, Multi-parametric assessment of cardiomyocyte excitation-contraction coupling using impedance and field potential recording: a tool for cardiac safety assessment, *J. Pharmacol. Toxicol. Methods* 81 (2016) 201–216, <https://doi.org/10.1016/j.jvasc.2016.06.004>.
- [53] M.K. Jonsson, Q.D. Wang, B. Becker, Impedance-based detection of beating rhythm and proarrhythmic effects of compounds on stem cell-derived cardiomyocytes, *Assay. Drug Dev. Technol.* 9 (2011) 589–599, <https://doi.org/10.1089/adt.2011.0396>.
- [54] J. Tamargo, R. Caballero, R. Gómez, C. Valenzuela, E. Delpón, Pharmacology of cardiac potassium channels, *Cardiovasc. Res.* 62 (2004) 9–33, <https://doi.org/10.1016/j.cardiores.2003.12.026>.
- [55] C.N. Toepfer, A. Sharma, M. Cicconet, A.C. Garfinkel, M. Mücke, M. Neyazi, J. A. Wilcox, R. Agarwal, M. Schmid, J. Rao, J. Ewald, SarcTrack: an adaptable software tool for efficient large-scale analysis of sarcomere function in hiPSC-cardiomyocytes, *Circ. Res.* 124 (2019) 1172–1183, <https://doi.org/10.1161/CIRCRESAHA.118.314505>.
- [56] G.Y. Oudit, H. Sun, M.G. Trivieri, S.E. Koch, F. Dawood, C. Ackerley, M. Yazdanpanah, G.J. Wilson, A. Schwartz, P.P. Liu, P.H. Backx, L-type Ca²⁺ channels provide a major pathway for iron entry into cardiomyocytes in iron-overload cardiomyopathy, *Nat. Med.* 9 (2003) 1187–1194, <https://doi.org/10.1038/nm920>.
- [57] D.M. Bers, Cardiac excitation-contraction coupling, *Nature* 415 (2002) 198–205, <https://doi.org/10.1038/415198a>.
- [58] W.S. Redfern, L. Carlsson, A.S. Davis, W.G. Lynch, I.L. MacKenzie, S. Palethorpe, P. K.S. Siegl, I. Strang, A.T. Sullivan, R. Wallis, Camm, A.J., Relationships between preclinical cardiac electrophysiology, clinical qt interval prolongation and torsade de pointes for a broad range of drugs: evidence for a provisional safety margin in drug development, *Cardiovasc. Res.* 58 (2003) 32–45, [https://doi.org/10.1016/s0008-6363\(02\)00846-5](https://doi.org/10.1016/s0008-6363(02)00846-5).

Ms. Yuyan Liu is a Ph.D. student at the MEMS and Nanotechnology laboratory, Mechanical engineering department at Chonnam National University. Her research activity is primarily focused on developing MEMS-based biosensing platforms for biomedical applications.

Dr. Nomin-Erdene Oyunbaatar obtained her Ph.D. degree in 2018 from department of Mechanical Engineering, Chonnam National University, Korea. She is currently working as post-doctoral researcher at MEMS and Nanotechnology Laboratory of Chonnam National University, Korea. Her current research interests include Bio-sensors based on MEMS and smart stent

Dr. Arunkumar Shanmugasundaram completed his Ph.D from CSIR-Indian Institute of Chemical Technology, Hyderabad, India. Currently he is working as a post-doctoral researcher at MEMS and Nanotechnology laboratory, School of Mechanical Engineering,

Chonnam National University, Korea. His research interests include design and development of next generation sensors for biomedical applications.

Prof. Eung-Sam Kim received his Ph.D in School of Interdisciplinary Bioscience and Bioengineering from Pohang University of Science and Technology (POSTECH), Pohang, Korea in 2011. Currently, he is working as a professor at Department of Biological Sciences, Chonnam National University, Korea, with research interests in cell mechanotransduction and biology-inspired nanosystems.

Prof. Bong-Kee Lee received his Ph.D in Mechanical Engineering from Pohang University of Science and Technology (POSTECH), Pohang, Korea. Currently he is working as a professor at School of Mechanical Engineering, Chonnam National University, Korea. His

research interests lie in a development of advanced micro/nano molding technologies and their application in optical, microfluidic, and biomedical areas.

Prof. Dong-Weon Lee received his Ph.D. degrees in Mechatronics engineering from Tohoku University, Sendai, Japan in 2001. He has been a Professor of Mechanical Systems Engineering at Chonnam National University (CNU), South Korea since 2004. Previously, he was with the IBM Zurich Research Laboratory in Switzerland, working mainly on microcantilever devices for chemical AFM applications. At CNU, his research interests include smart cantilever devices, miniaturized energy harvester, smart structures & materials, and nanoscale transducers. He is a member of the technical program committee of IEEE Sensors Conference, Transducers, and Microprocesses and Nanotechnology Conference.